

## HYDRODYNAMIC SIMULATION AND SPECTRA DETERMINATION IN AQUEOUS $H_2SO_4$ SOLUTIONS CAVITATION BUBBLES

**Pablo L. García Martínez, Gabriela F. Puente, Fabián J. Bonetto**

Laboratorio de Cavitación y Biotecnología  
Instituto Balseiro, Centro Atómico Bariloche  
Av. Bustillo 9500, 8400, Bariloche, Argentina  
e-mail: garciamp@ib.cnea.gov.ar

**Keywords:** Sonoluminescence, Compressible flow, Spectra.

### **Abstract.**

*Light emission in single-bubble sonoluminescence (SBSL) experiments results from the extreme conditions reached during the very strong collapse of a gas bubble driven into non-linear radial oscillations. Recent experiments achieved an important enhancement (by a factor 2700) in the light emitted from the bubble by using Argon bubbles within aqueous  $H_2SO_4$  solutions.<sup>1</sup> The very marked increase in SBSL intensity allowed well resolved spectra determination revealing the presence of spectral lines coming from atomic (Ar) emission and other molecular and ionic processes.*

*In the present work we calculate the hydrodynamic motion of the gas inside the bubble using compressible Navier-Stokes equations in spherical symmetry in order to obtain instantaneous temperature and density profiles. Taking the previous results as input we apply a spectral model which incorporates atomic physics and takes into account the finite opacity of the gas under the extreme conditions at bubble collapse. Results are in agreement with timescale of the light pulse width and continuum part of experimental spectra measured.<sup>1</sup> Besides we found that brighter bubbles are not necessarily hotter bubbles. The full model presented constitutes an adequate starting point for modelling line emission observed in experiments.*

## 1 INTRODUCTION

Single-bubble sonoluminescence (SBSL) occurs when an acoustically trapped and periodically driven gas bubble collapses so strongly that the energy focusing at collapse leads to light emission. Up to now, no experimental determination of the conditions prevailing in the bubble's interior, like temperature or pressure, has been achieved. For this reason modelling plays a major role in understanding the phenomenon. While the most crucial variable to determine is the gas temperature during the collapse, the two more important measurable quantities in SBSL are the bubble radius and the light intensity.<sup>2</sup>

In this communication we describe a complete detailed model for the dynamics of the bubble which from first principles reproduces the motion of the interface liquid-gas, detailed hydrodynamic conditions inside the bubble and the volumetric light emission process, taking experimental conditions as the input data. Thus, comparison with experiment may be performed for the resulting interface dynamics and also the light pulse emitted, giving more confidence to temperature estimations (if such experimental data were available for H<sub>2</sub>SO<sub>4</sub> solutions).

Motivated by recent experimental results that achieved an important light emission enhancement<sup>1</sup> we apply our model to Argon bubbles under Sulfuric acid, which besides constitutes an important simplification because the low vapor pressure of the Sulfuric acid makes possible to neglect chemical processes due to vapor inside the bubble.

## 2 MODEL DESCRIPTION

The model used for the estimation of light emission consists of two parts. The first one is the hydrodynamic model of the gas inside the bubble accomplished by an equation for the bubble radius describing the dynamics of the gas-liquid interface. Once the conditions inside the bubble have been determined, a model for light emission which incorporates finite opacity of the hot gas and takes into account the spatial dependence of temperature and density is applied.

### 2.1 Hydrodynamic Model

We begin on describing the hydrodynamic model and the motion of the interface. The non-linear dynamics of the interface of a highly forced bubble is well reproduced by the Keller-Miksis formulation of the Rayleigh-Plesset equation<sup>3</sup>

$$\left(1 - \frac{\dot{R}}{c_l}\right) \rho_l R \ddot{R} + \frac{3}{2} \dot{R}^2 \rho_l \left(1 - \frac{\dot{R}}{3c_l}\right) = \left(1 + \frac{\dot{R}}{c_l}\right) (p_g - p_a - p_\infty) + \frac{R}{c_l} \dot{p}_g - 4\eta \frac{\dot{R}}{R} - \frac{2\sigma}{R}, \quad (1)$$

where  $R$ ,  $\dot{R}$  and  $\ddot{R}$  are the radius, velocity and acceleration of the bubble interface,  $\rho_l$ ,  $c_l$  and  $\eta$  are the density, sound speed and viscosity of the surrounding liquid,  $\sigma$  is the surface tension of the gas-liquid interface,  $p_g$  is the gas pressure (inside the bubble),  $p_a$  is the acoustic pressure (imposed by ultrasonic field) and  $p_\infty$  is the atmospheric pressure.

Modelling the behavior of the gas inside the bubble is a necessary requirement for obtaining  $p_g$  and closing (1). Different levels of sophistication may be introduced at this stage. An

approximation often made assumes uniform pressure and uses some equation of state for the gas and some simplified model to take into account heat exchange between gas and liquid.<sup>4</sup> Instead, in this work we use a detailed hydrodynamic model capable of reproducing the spatial profiles of gas temperature, pressure, etc. inside the bubble. To this end we solve the full system of compressible Navier-Stokes equations neglecting fluid viscosity and assuming spherical symmetry,

$$\begin{aligned} \frac{\partial \rho}{\partial t} + \frac{\partial(\rho u)}{\partial r} &= -\frac{2}{r}(\rho u), \\ \frac{\partial}{\partial t}(\rho u) + \frac{\partial}{\partial r}(\rho u^2 + p) &= -\frac{2}{r}(\rho u^2), \\ \frac{\partial E}{\partial t} + \frac{\partial}{\partial r}[(E + p)u] &= -\frac{2}{r}[(E + p)u] + \frac{1}{r^2} \frac{\partial}{\partial r} \left( r^2 k \frac{\partial T}{\partial r} \right), \end{aligned} \quad (2)$$

where  $\rho$ ,  $u$ ,  $T$  and  $p$  are the gas density, radial velocity, gas temperature and pressure respectively,  $E = \rho u^2/2 + \rho e$ , is the total energy per unit volume,  $e$  is the specific internal energy, and  $k$  is the thermal conductivity assumed linear in  $T$ ,  $k(T) = k_\infty T/T_\infty$ . Closing (2) requires an equation of state (EOS) for the gas. Algebraic formulas for the pressure  $p$  and the internal energy  $e$  of mono atomic fluids as functions of density and temperature ( $p[\rho, T]$  and  $e[\rho, T]$ ) are employed.<sup>5</sup>

The change of coordinates given by  $x \equiv r/R(t)$  is used to transform the gas dynamics equations (2) into a form in a fixed domain  $x \in [0, 1]$ .<sup>6</sup> Explicit time MacCormack's predictor-corrector<sup>7</sup> is used to advance the advective terms of resulting system. The diffusive term coming from heat exchange is treated explicitly.

## 2.2 Light emission model

The simplest approach one can think of is the ideal blackbody model in which case the gas is assumed to be a perfectly photon absorber and to emit a spectral intensity (energy per unit time, wavelength interval, solid angle and projected surface area) at wavelength  $\lambda$  given by the Planck's law,

$$I_\lambda^{Pl} = \frac{2hc^2}{\lambda^5 [\exp(hc/\lambda k_B T) - 1]}, \quad (3)$$

with the Planck and Boltzmann constants  $h$  and  $k_B$ , and the speed of light in vacuum  $c$ . In the work of Hilgenfeldt *et. al.*<sup>8</sup> this assumption was analyzed in conduction with a model of uniform pressure and temperature for the bubble interior and they found that it fails in describing properly basic features of bubble spectra like pulse duration at different wavelength intervals, spectral shape and, less importantly, total power emitted. They also proposed a refinement of the model incorporating a finite opacity model for the bubble arguing that in contrast with blackbody infinite opacity the gas is transparent to its own radiation almost all the time. This

idea leads to the interpretation of the bubble as a volume emitter (optically thin) instead of a surface emitter (optically thick).

We denote by  $\kappa_\lambda[T(s, t)]$  the photon absorption coefficient (the inverse of the photon mean free path), which depends on the wavelength,  $\lambda$ , and, via temperature,  $T$ , on the location within the bubble,  $s$ , and the time,  $t$ . Then, the emitted intensity, at wavelength  $\lambda$ , with a thickness  $s$  of the medium is

$$I_\lambda(s, t) = \int_0^s \kappa_\lambda[T(s', t)] \exp\left(-\int_0^{s'} \kappa_\lambda[T(s'', t)] ds''\right) I_\lambda^{Pl}[T(s', t)] ds'. \quad (4)$$

Using the uniform temperature assumption it is possible to derive analytically an equation for the total spectral power emitted.<sup>8</sup> Nevertheless, we shall leave (4) in this form in order to perform the integral numerically using the calculated temperature profiles. Numerical integration is done following elementary algorithms for extended trapezoidal rule.<sup>9</sup>

To determine the photon absorption coefficient from calculated conditions inside the bubble, dominant microscopic photon absorption processes must be identified. We use the approximation introduced by Hilgenfeldt *et. al.*,<sup>8</sup> which is  $\kappa_\lambda = \kappa_\lambda^{ff0} + \kappa_\lambda^{\text{ion}}$ , where

$$\kappa_\lambda^{ff0}(T) = \frac{e^2}{\pi \epsilon_0} \frac{(2k_B T)^{9/4} n^{3/2}}{h^{3/2} c^3 m_e^{3/4} \pi^{3/4}} \lambda^2 \left( c_{tr} + \frac{d_{tr}}{3k_B T} \right) \exp\left(-\frac{E_{\text{ion}}}{2k_B T}\right), \quad (5)$$

$$\kappa_\lambda^{\text{ion}}(T) = \frac{16\pi^2}{3\sqrt{3}} \frac{e^6 k_B T n}{(4\pi \epsilon_0)^3 h^4 c^4} \lambda^3 \exp\left(-\frac{E_{\text{ion}} - hc/\max[\lambda, \lambda_2]}{k_B T}\right), \quad (6)$$

where the constants  $e$ ,  $\epsilon_0$ ,  $E_{\text{ion}}$  are electron charge, the vacuum permeability and the ionization energy, and  $n$  is the number density of atoms.

Interactions of photons with electrons colliding inelastically with neutral atoms is taken into account by  $\kappa_\lambda^{ff0}$  in (5), where the constants  $c_{tr} \approx 1.6 \times 10^{-20} \text{m}^2/\text{eV}$  and  $d_{tr} \approx -0.6 \times 10^{-20} \text{m}^2$  come from an approximation for the effective inelastic collision cross section of electrons with neutral atoms.

Equation (6) gives the absorption coefficient for two processes ( $\kappa_\lambda^{\text{ion}} = \kappa_\lambda^{bf} + \kappa_\lambda^{ff+}$ ): the photonic *bound-free* ionization of already excited atoms and the photon absorption coefficient due to *free-free* interactions of electrons and ions. The wavelength  $\lambda_2 = 292 \text{nm}$  corresponds to the lowest-lying level above the ground state.

Apart from the three processes considered above it also exists an additional contribution due to *bound-bound* excitations of electrons on the discrete energy levels of the atom, which is responsible for line emission observed in SBSL.<sup>1</sup> As this effect is the hardest to model we leave it for future work, and we concentrate in the continuous part of the spectra.

Identifying the photon absorption mechanisms automatically determines the emission mechanisms, as a consequence of Kirchhoff's law, which states that absorption and emission are reciprocal processes. Thus, the primary processes for the continuum emission of SBSL are precisely inverse to those responsible for absorption: (i) bremsstrahlung from inelastic collisions

of free electrons with neutral atoms ( $\kappa_{\lambda}^{ff0}$ ); (ii) bremsstrahlung of electrons in the field of ions ( $\kappa_{\lambda}^{ff+}$ ); and (iii) photon emission from recombination of free electrons and ions to form excited atoms ( $\kappa_{\lambda}^{bf}$ ).

### 3 RESULTS AND DISCUSSION

When defining experimental conditions one fixes most of the parameters involved in the model described before. For example, physical properties of the gas and the liquid are obviously defined by choosing Argon and Sulfuric acid solution, driving frequency is determined by the resonator (in conjunction with the acoustic properties of the liquid), and ambient parameters (i.e. liquid temperature and external pressure) may be simply lab ambient conditions or others specifically imposed. In this work we use 30 kHz for the driving frequency, and lab atmospheric conditions, 0.92 atm and 300°K.

The parameters that remain free and define the parameter space of SBSL are the acoustic pressure  $p_{ac}$  and the ambient radius  $R_0$ . The former corresponds to the ultrasonic stationary field amplitude and the latter is the radius that would have the bubble unforced at normal conditions (T=273°K, and p=1atm). In order to explore this parameter space we follow the curves of diffusive stable equilibrium, which meaning can be explained as follows. As gas diffuses into and out of the bubble some dynamical stable equilibrium must be reached in the region of parameter space where stable bubbles are observed (no net mass exchange). In this region each curve of stability, corresponding to a fixed dissolved gas concentration in the liquid, tell us which  $R_0$  (so which amount of gas mass) satisfies the diffusive equilibrium at a given  $p_{ac}$ . Using the model described in Ref. [10] for the diffusive stability, the curves for different gas concentrations showed in Fig. 1 are obtained.

After determining the region of interest we choose one point in  $(p_{ac}, R_0)$  space to show how

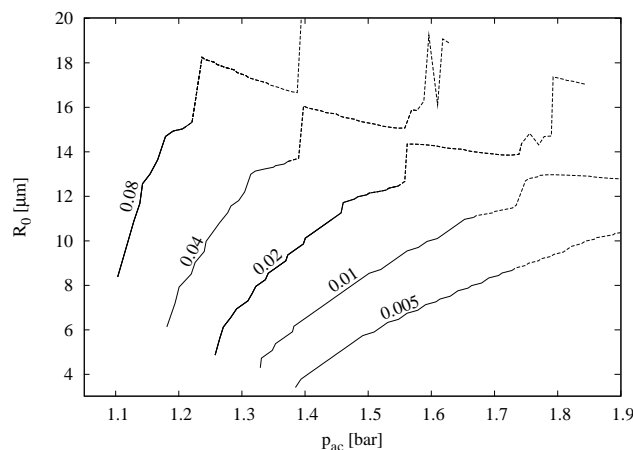


Figure 1: Curves of diffusive stability for Argon bubbles in  $H_2SO_4$  solution for various dissolved gas concentrations. Concentrations are expressed relative to saturation concentration ( $c_{\infty}/c_{sat}$ ). Curves are drawn with dashed lines where some kind of instability is likely to extinct the bubble (e.g. Rayleigh-Taylor, parametric, Bjerknes, etc.).

typical results of the model described in the precedent section look like. In Fig. 2 we can see the temporal evolution of central temperature, bubble radius and calculated light emission intensity (left), and also temperature profiles as a function of the radial coordinate (right), during the collapse.

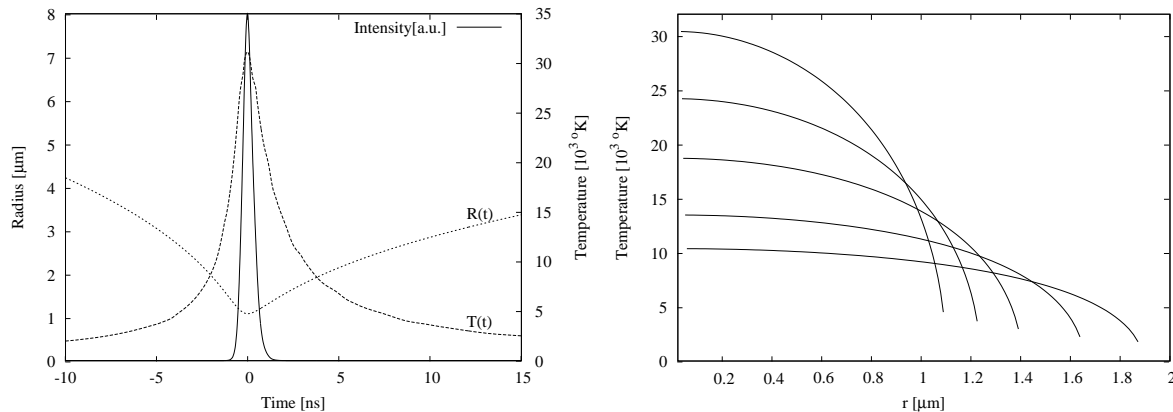


Figure 2: Results for a typical case, with  $p_{ac} = 1.45$  bar and  $R_0 = 7.7\mu\text{m}$ . On the left, central temperature,  $T(t)$ , bubble radius,  $R(t)$ , and light intensity are depicted. On the right, internal spatial temperature profiles.

Light emission takes place when some portion of the gas inside the bubble reaches temperatures above  $10000^\circ\text{K}$ , as seen in Fig. 2, resulting in an extremely short light pulse (hundred of picoseconds). We can also see that temperature inside the bubble is not uniform but smooth which implies that we can discard shock-wave theory of SBSL.<sup>11</sup> Besides, as a consequence of the non uniform temperature profile we could expect different results when assuming uniform temperature<sup>8</sup> or when taking into account the calculated profiles, provided that the mechanisms of light emission described rely on the degree of ionization which grows exponentially with temperature. Fig. 3 shows two sets (at  $p_{ac} = 1.3$  bar and  $p_{ac} = 1.8$  bar for 0.01 of relative gas concentration) of three calculated spectra using three different levels of approximation: (i) detailed calculation performing integral (4) using temperature and density profiles (solid lines), (ii) assuming transparent uniform temperature bubble<sup>8</sup> (dashed), and (iii) assuming uniform temperature and blackbody radiation (dotted).

It is possible to observe in Fig. 3 that, as expected, taking into account the spatial dependence of temperature leads to more intense calculated emission than uniform models, due to higher temperatures considered, notwithstanding, blackbody model is still the brightest. We also note that at relative low pressures ( $p_{ac} = 1.3$ ) the detailed model is more similar to the uniform model, but at stronger driving and higher temperatures the detailed model is more similar to a blackbody.

Comparison of spectra calculated with spectra measurements performed in Ref. [1] leads to the following observations. Firstly, the range of intensity measured is in accordance with our calculations of emission for bubbles under typical conditions of  $(p_{ac}, R_0)$  showed by solid lines of Fig. 1. Note that 1.3 bar of the 0.01 curve of Fig. 1 is rather low and its spectral radiant

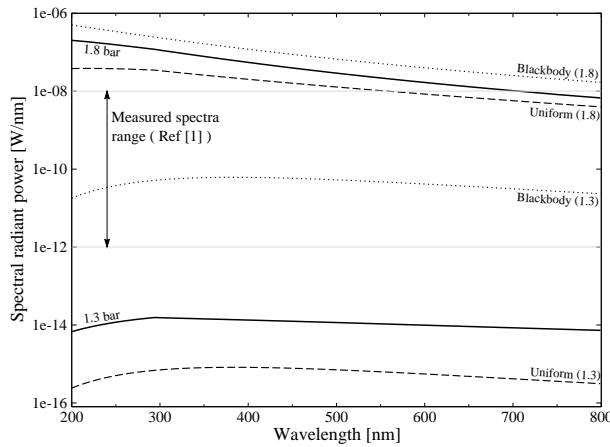


Figure 3: Spectral radiance of emitted SL light (averaged over one period). Solid lines correspond to detailed spatial model for 1.3 bar and 1.8 bar. Dashed lines are the results from uniform temperature model<sup>8</sup> and dotted, from blackbody model.

power falls under the measurement range, while 1.8 bar is very high and its respective emission is more intense than measurements. Spectral radiant power resulting from intermediate values of acoustic pressure fall between solid lines of Fig. 3. This fact suggests that the upper limits for the acoustic pressure reported by Ref [1] (2.3 bar to 5.5 bar) are too overestimated. Secondly, spectral shape produced by the model is in agreement with experimental observations in the UV and part of the visible. Lastly, the presence of line emission in the infrared part of the experimental spectrum leads to the necessity of including a fourth emission mechanism, taking into account *bound-bound* excitations of electrons.

Predicted total power emitted as a function of acoustic pressure for different dissolved gas concentrations is shown in Fig. 4. The total power emitted increases with increasing acoustic pressure in the considered range faster than linearly but slower than exponentially. Corresponding bubble maximum averaged temperatures are plotted in Fig. 5.

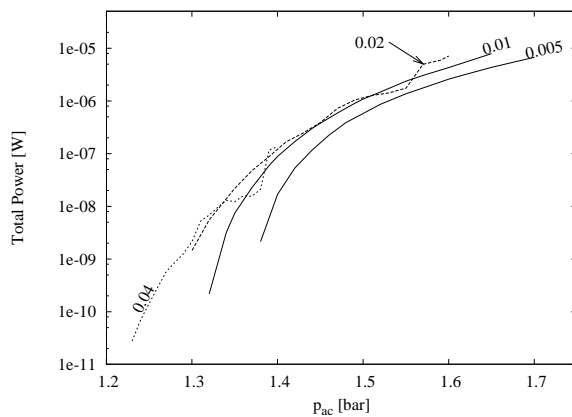


Figure 4: Total emitted power in watts as a function of acoustic pressure for different dissolved gas concentrations.

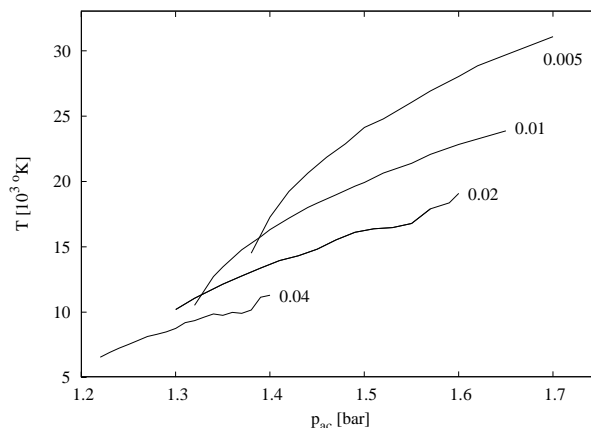


Figure 5: Maximum averaged gas temperature during the collapse as a function of acoustic pressure for different dissolved gas concentrations.

Note that maximum averaged temperatures are far lower than maximum central temperatures, as one can deduce by looking at the value for  $p_{ac} = 1.45$  and  $c_{\infty}/c_{sat} = 0.01$  in Fig. 5 (below  $20000^{\circ}\text{K}$ ), and the highest temperature showed in Fig. 2 (above  $30000^{\circ}\text{K}$ ).

Comparing power emitted and temperature it comes out a non intuitively result of the model used: brighter bubbles not necessarily implies hotter bubbles. The curve 0.005 of Fig. 4 is below the curve 0.01, but this order is inverted in the temperature plots of Fig. 5. Since light emission not depends only on temperature but also on bubble size and mass content, increasing the gas concentration leads to probably brighter bubbles because they are larger, not because they are hotter.

#### 4 CONCLUSIONS

We have presented a complete model for SBSL phenomenon including the gas dynamics inside the bubble, the liquid-gas interface dynamics and the light emission processes. It satisfactorily reproduces the time scales associated with the two observables of SBSL: the interface motion and the light pulse emitted. It also gives quantitative good results when compared with the continuum part of the measured light emission spectra,<sup>1</sup> but we remark on the few availability of data for aqueous  $\text{H}_2\text{SO}_4$  solutions and the necessity of further comparison against experimental observations. We also point out the importance of extending the light emission model to incorporate line emission coming from the decay of excited Argon atoms, in order to identify the processes responsible for that kind of observations. In that sense, the scheme presented here may be seen as the necessary starting point to model the more complicated physics underlying infrared line emission observed, a process not yet clearly understood inside the bubble.

As a first preliminary result of the model we found a not straight forward relationship between maximum temperature achieved by the bubble and intensity of light emission, because the latter depends also on bubble size and mass content. This may be a relevant fact when searching higher temperatures inside the bubble.

## REFERENCES

- [1] Flannigan, D.J., and Suslick, K.S., D., 2005, "Plasma formation and temperature measurement during single-bubble cavitation", *Nature*, **434**, pp. 52-55.
- [2] Brenner, M.P., Hilgenfeldt, S., and Lohse, D., 2002, "Single-bubble sonoluminescence", *Rev. Mod. Phys.*, **74**, pp. 425-483.
- [3] Keller, J.B., and Miksis, M.J., 1980, "Bubble oscillations of large amplitude", *J. Acoust. Soc. Am.* **68**, pp. 628.
- [4] Toegel, R., Gompf, B., Pecha, R., and Lohse, D., 2000, "Does water vapor prevent upscaling sonoluminescence?", *Phys. Rev. Lett.*, **85**, pp. 3165-3168.
- [5] Vuong, V.Q., Szeri, A.J., and Young, D.A., 1999, "Shock formation within sonoluminescence bubbles", *Phys. Fluids*, **11**, pp. 10-17.
- [6] Yuan, L., Cheng, H., Chu, M., Leung, P., 1998, "Physical parameters affecting sonoluminescence: A self-consistent hydrodynamic study", *Phys. Rev. E*, **57**, pp. 4265-4279.
- [7] Leveque, R.J., 2002, *Finite Volume Methods for Hyperbolic Problems*, Cambridge University Press, Cambridge, UK.
- [8] Hilgenfeldt, S., Grossmann S., Lohse, D., 1999, "Sonoluminescence light emission", *Phys. Fluids*, **11**, pp. 1318-1330.
- [9] Press, W., Vetterling, W., Teulosky, S., Flannery, B., 1992, "Numerical Recipes in FORTRAN 77", Cambridge Univ. Press.
- [10] Puente, G., Urteaga, R., Bonetto, F., 2005, "Numerical and experimental study of dissociation in an air-water single-bubble sonoluminescence system", *Phys. Rev. E*, **72**, pp. 1-10.
- [11] García Martínez, P., Bonetto, F., 2004, "Simulación numérica de ondas de presión y de choque en sonoluminiscencia utilizando esquemas de upwind", *Mec. Computacional*, **XXIII**, pp. 2735-2743.